Electronic Supplementary Information

Synthesis and optical properties of emission-tunable PbS/CdS core-shell quantum dots for *in vivo* fluorescence imaging in the second near-infrared window

*Yoshikazu Tsukasaki,[a] Masatoshi Morimatsu,[b], Goro Nishimura,[c] Takao Sakata,[d] Hidehiro Yasuda,[d] , Akihito Komatsuzaki,[a] Tomonobu M.Watanabe[a,b,e] and Takashi Jin *[a,b,e]*

[a] *RIKEN Quantitative Biology Center, 6-2-3 Furuedai, Suita, Osaka 565-0874, Japan.*
[b] *Graduate School of Frontier Biosciences, Osaka University, Yamada-oka 2-1, Suita, Osaka 565-0871, Japan.*
[c] *Research Institute for Electronic Science, Hokkaido University, N20W10, Sapporo 001-0020, Japan.*
[d] *Research Center for Ultra-High Voltage Electron Microscopy, Osaka University, Mihogaoka 7-1, Ibaraki, Osaka 567-0047, Japan.*
[e] *Immunology Frontier Research Center, Osaka University, Yamada-oka 1-3, Suita, Osaka 565-0871, Japan.*
E-mail: tjin@riken.jp

Experimental description

Cell viability test for BSA-conjugated PbS/CdS QDs

HeLa cells were incubated at different times and different BSA-coated PbS/CdS QDs concentrations. After incubation for 30 min, cells were washed and resuspended in a culture media (DMEM). A 10 μL of the cell suspension was mixed with a Trypan blue solution (10 μL), and the cell viability was determined using a cell counter (Countess; Invitrogen).

Monte Carlo simulation of VIS, 1st-NIR and 2nd-NIR imaging

Fluorescence images of microspheres were simulated by Monte Carlo simulations. The algorithm essentially followed Wang's method.[1)] In our simulation, the sphere light source was located at the fluorescent microsphere and the trajectory in the tissue was calculated using the Monte Carlo method. The microscopic image of the microsphere was generated by calculating the photon position at the focused plane where the center position of the microsphere was located using the reverted direction and position of the exit photons from the glass surface. Thus, the optics in the simulation always focused the sphere with infinitely accurate resolution. The photon was discretized into two states: alive and dead.

The simulation was performed for a tissue sample enclosed between two glass cover slips (G1, G2) with a thickness of 0.17 mm. A photon was generated from an arbitrary position inside a microsphere placed at the origin of the xy-plane and a depth, z, from the glass slide. The initial direction of a photon was isotropic, and 5×10^9 photons were generated in the simulation. A photon was traced until it was absorbed by the tissue, exited the boundary, or travelled beyond 20 cm. Exit photons were collected by the objective lens whose focal length and diameter were 28.57 mm and 14.28 mm, respectively. If a photon reached outside the lens or had a large directional angle relative to the normal direction of the lens, i.e. larger than the arc tangent of the numerical aperture (0.259), the photon was discarded. The image was reconstructed at the focus plane (*op*), because that is where we assumed the lens was focused. The number of photons focused in each 2.5 μm × 2.5 μm area in the focus plane was counted. Optical parameters of the glass cover slip were as follows: scattering coefficient, 0.001 mm^{-1}; absorption coefficient, 0.0001 mm^{-1}; anisotropy, 1.0; and refractive index, 1.52. Optical parameters of the tissue, μ_s and μ_a, were given typical values acquired from spectrometer measurements with an integrating sphere (see, Table 1), and the refractive index (n) and the anisotropy (g) were fixed at 1.34 and 0.9, respectively. The program code was based on CUDAMCML code originally developed by the Lund group [2] (http:/www.atomic.physics.lu.se/fileadmin/atomfysik/Biophotonics/Software/CUDAMCML.zip), but customized for our application.

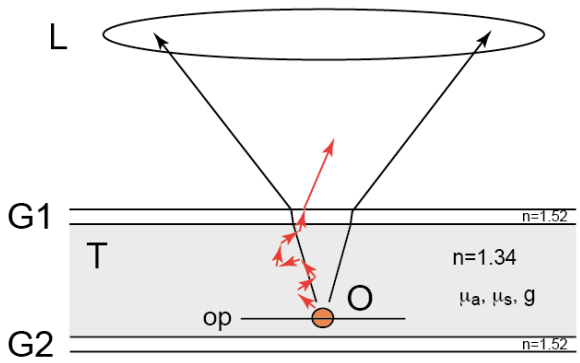

Figure 1. The simulation geometry of Monte Carlo simulation. The photon source (O) in a tissue sample (T) enclosed by two glass cover slips (G1, G2) and the photon random walk (red arrows) is traced by a Monte Carlo simulation. The exit photon is collected by a lens (L) and focused onto the image plane. *op*, focus plane.

(a) Brain optical property parameters

	μ_t (mm^{-1})	Penetration depth (mm)	Ratio	μ_a (mm^{-1})	μ_s (mm^{-1})
482	18.162	0.055		0.698	17.465
520	16.714	0.060		0.935	15.776
670	11.693	0.086		0.300	11.391
720	10.520	0.095		0.268	10.255
785	9.272	0.108		0.252	9.023
1100	5.675	0.176		0.157	5.512
1300	4.657	0.215		0.496	4.156
1500	6.408	0.156		4.551	1.847
482+520	34.879	0.029	1		
670+720	22.212	0.045	1.57		
785+1000	14.941	0.067	2.33		
785+1300	13.932	0.072	2.50		
785+1500	15.673	0.064	2.23		

(a) Heart optical property parameters

	μ_t (mm^{-1})	Penetration depth (mm)	Ratio	μ_a (mm^{-1})	μ_s (mm^{-1})
482	11.211	0.089		2.101	9.104
520	11.135	0.090		2.799	8.331
670	9.542	0.105		0.754	8.783
720	8.898	0.113		0.579	8.306
785	8.092	0.124		0.496	7.591
1100	5.026	0.199		0.222	4.799
1300	4.072	0.188		0.448	3.623
1500	5.333	0.156		4.424	0.907
482+520	22.343	0.029	1		
670+720	18.424	0.045	1.25		
785+1000	13.110	0.067	2.22		
785+1300	12.164	0.072	2.73		
785+1500	13.427	0.064	2.09		

Table 1. Tissue optical properties measured by a spectrometer with an integrating sphere. μ_t, μ_a, and μ_s are the mean attenuation coefficients, absorption coefficients, and scattering coefficients, respectively. Penetration depth is defined as $1/\mu_t$. Ratio describes the penetration depth normalized to that at 482+520.

References

1) L. Wang, S. L. Jacques, L. Zheng, *Computer Methods and Programs in Biomedicine* 1995, **47**, 131.

2) E. Alerstam, T. Svensson, S. Andersson-Engels, *Journal of Biomedical Optics* 2008, **13**, 06504.

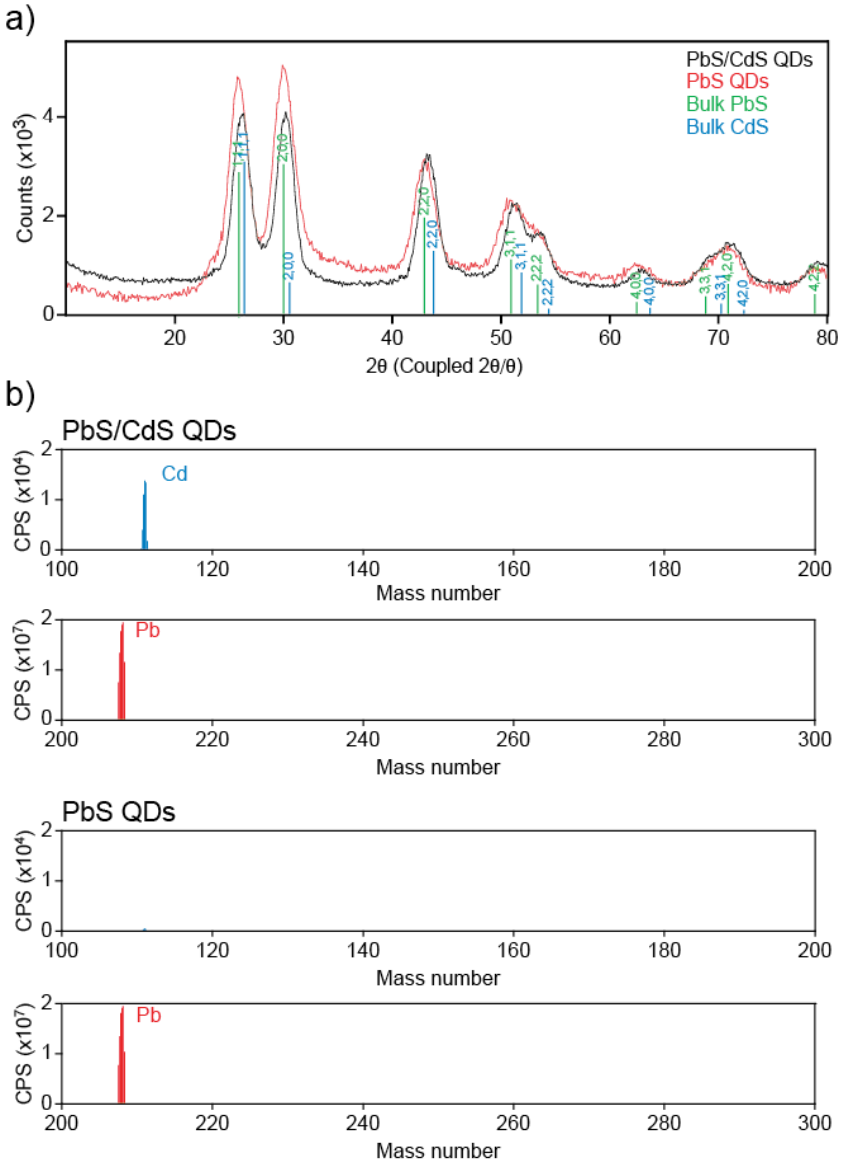

Fig. S1 a) XRD patterns of PbS/CdS QDs and PbS QDs with an emission wavelength of 1300 nm. Black and red curves are XRD patterns of PbS/CdS QDs and PbS QDs, respectively. Green and blue bars are the simulated results of bulk PbS and CdS, respectively. b) ICP-MS analysis of PbS/CdS QDs and PbS QDs with an emission wavelength of 1300 nm.

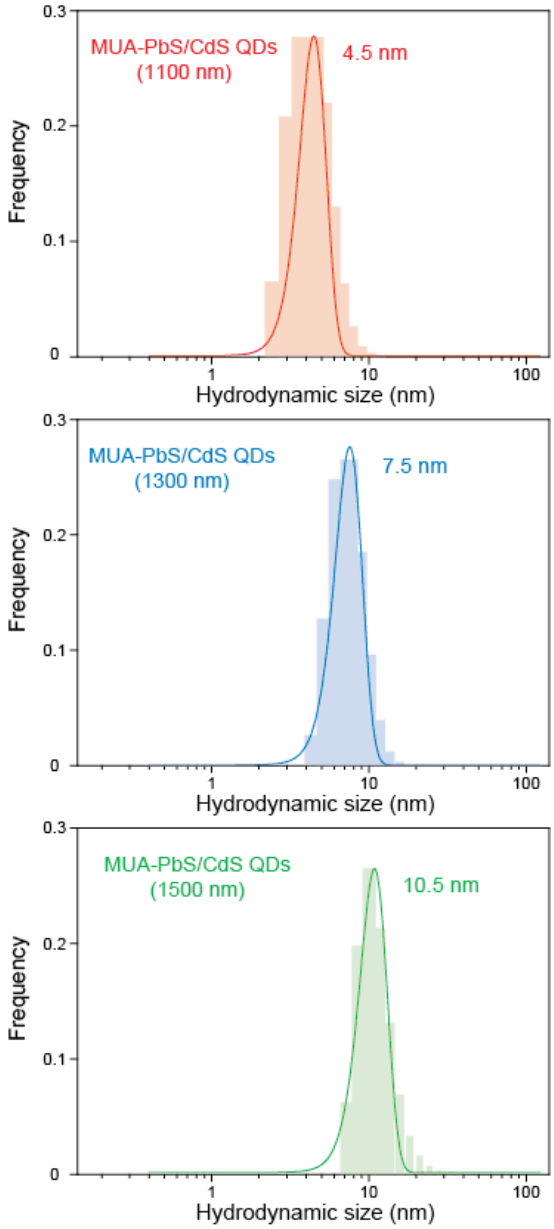

Fig. S2 Hydrodynamic diameter of MUA-coated PbS/CdS QDs (1100, 1300, and 1500 nm emission) in water. The diameters were determined by dynamic light scattering measurements.

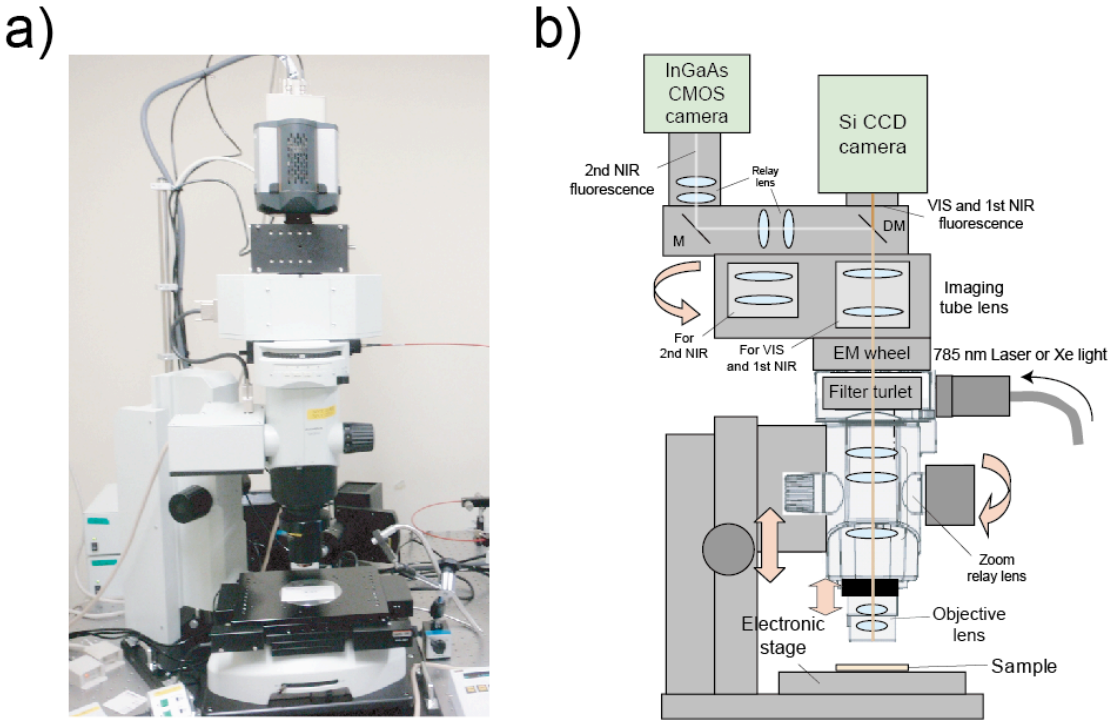

Fig. S3 Up-right fluorescence microscope system for *in vivo* imaging (400 -1500 nm) in VIS, 1st-NIR, and 2nd-NIR region.

(a) Brain optical property parameters

Ex/Em	μ_t (mm^{-1})	Penetration depth (mm)	Ratio
482/520	18.018	0.056	1
670/720	13.263	0.075	1.46
785/1000	7.105	0.141	2.54
785/1300	5.621	0.178	3.21
785/1500	9.291	0.108	1.94

(b) Heart optical property parameters

Ex/Em	μ_t (mm^{-1})	Penetration depth (mm)	Ratio
482/520	17.477	0.057	1
670/720	13.944	0.072	1.25
785/1000	12.796	0.078	1.37
785/1300	9.248	0.108	1.89
785/1500	13.426	0.074	1.3

Table S1 Optical properties of tissue slices measured by using VIS, 1st-NIR 2nd-NIR imaging. Ex/Em: excitation/emission wavelengths, μ_t: attenuation coefficients. Penetration depth is defined as $1/\mu_t$. Ratio describes the normalized penetration depth compared to that at 482/520.

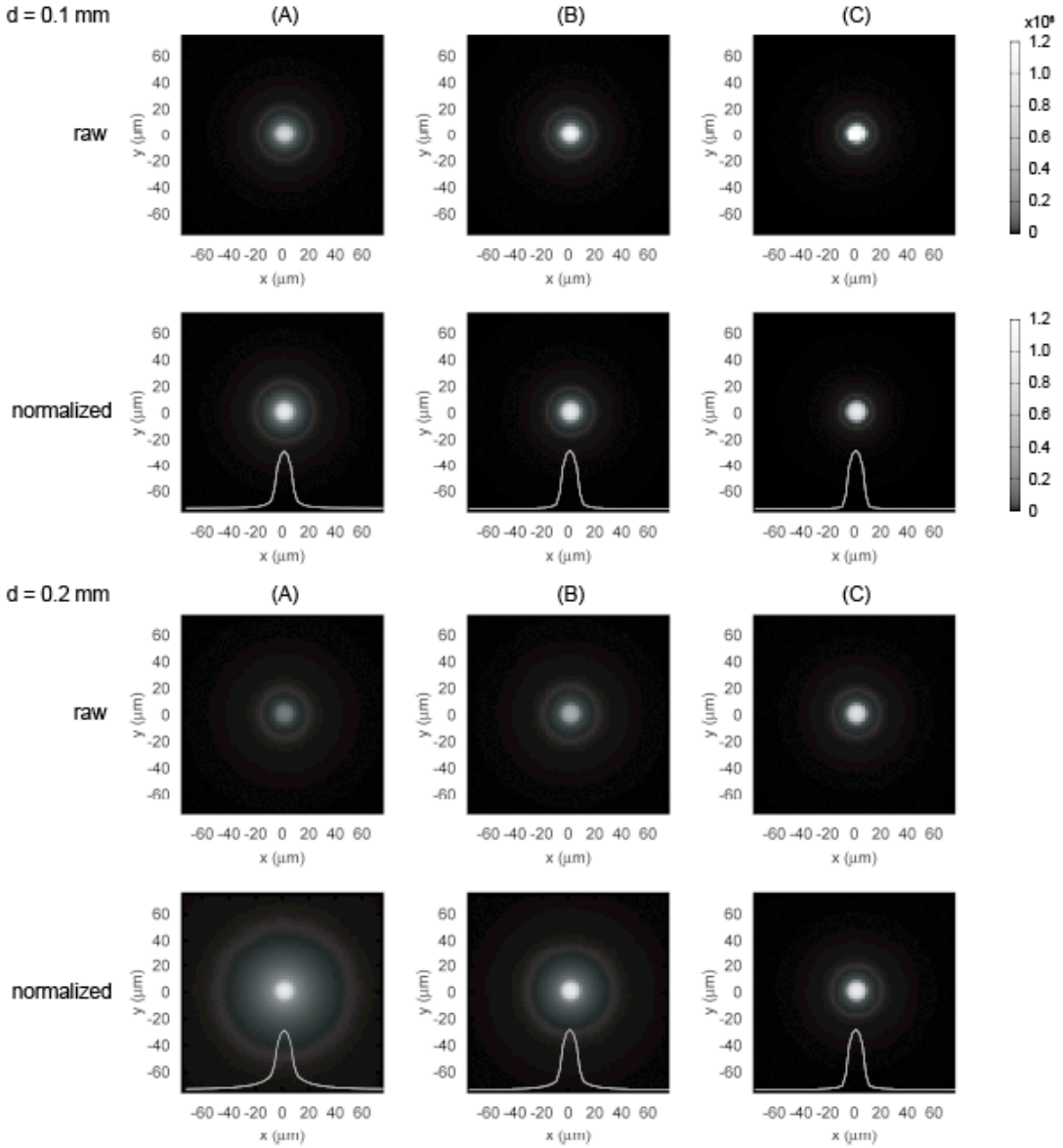
d = 0.1 mm
(A)
(B)
(C)
raw
normalized
d = 0.2 mm
(A)
(B)
(C)
raw
normalized
y (μm)
x (μm)
60
40
20
0
-20
-40
-60
-60 -40 -20 0 20 40 60
x10⁸
1.2
1.0
0.8
0.6
0.4
0.2
0

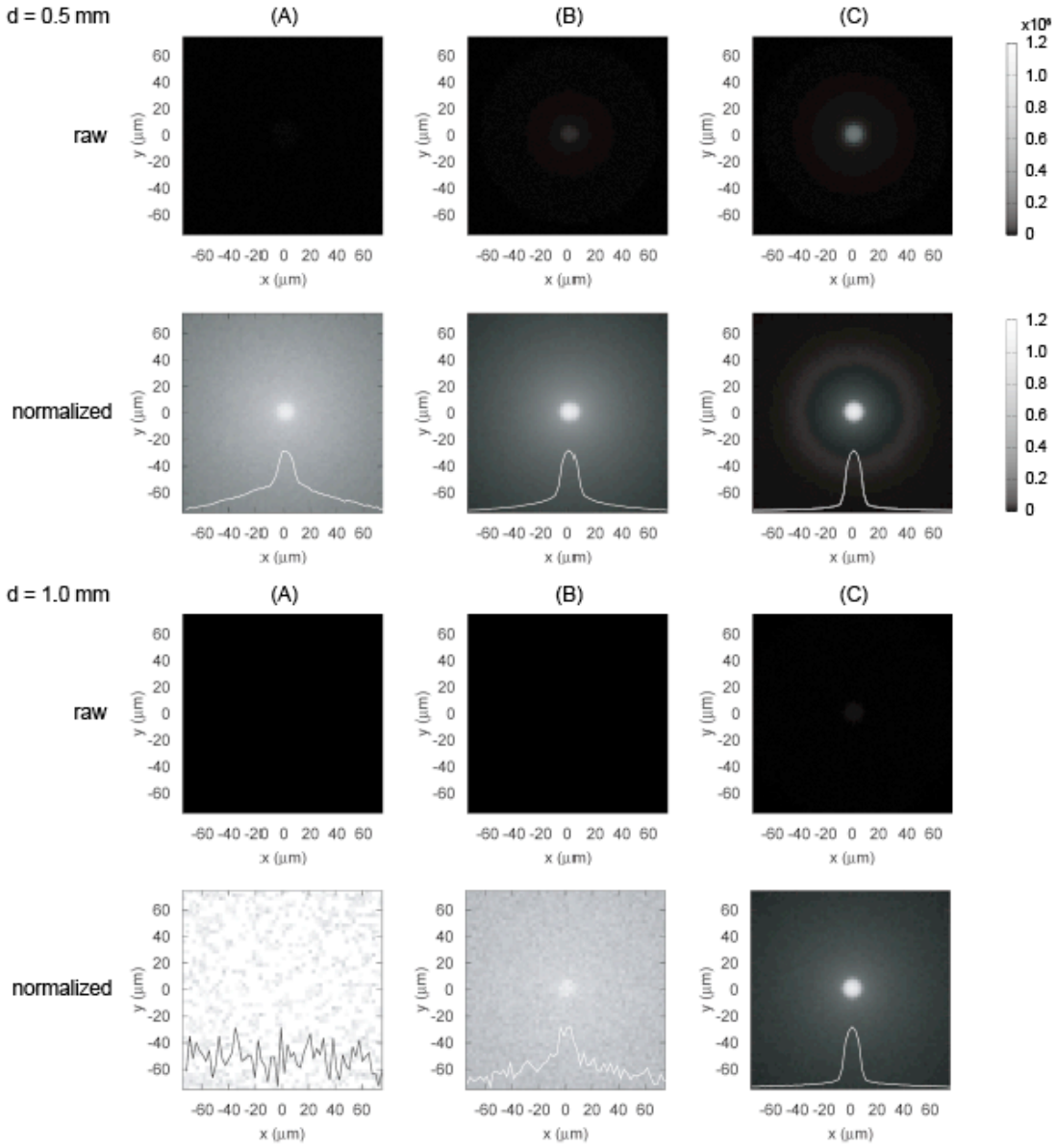

Fig. S4 Object images simulated by the Monte Carlo simulation at various optical parameter values and tissue thicknesses. Images are simulation results with sample thicknesses of 0.1, 0.2, 0.5 and 1.0 mm and (A) μ_s = 15 mm^{-1}, μ_a = 0.9 mm^{-1}, (B) μ_s = 10 mm^{-1}, μ_a = 0.268 mm^{-1} and (C) μ_s = 5 mm^{-1}, μ_a = 0.5 mm^{-1}, which are typical values for brain tissue, at emissions of 520, 720 and 1300 nm, respectively (Table 1). Each simulation is shown with two images, the raw image and the image normalized by the peak intensities. The cross section of the image at y = 0 m is shown in the normalized images. The brightness of the object in the raw image quickly diminished with the depth because of scattering and absorption. However, the object shape in the normalized

image was relatively maintained, as shown in the cross sections of the image. The intensities of the outside of the object significantly increased relative to the peak intensities with thickness, especially in the case of (A). This was because multiple scattering enhanced defocusing while ballistic photons, which form the object image, significantly decreased with higher scattering medium. The images are qualitative descriptions, with that at 1.3 μm being clearest and sharpest. d, depth.

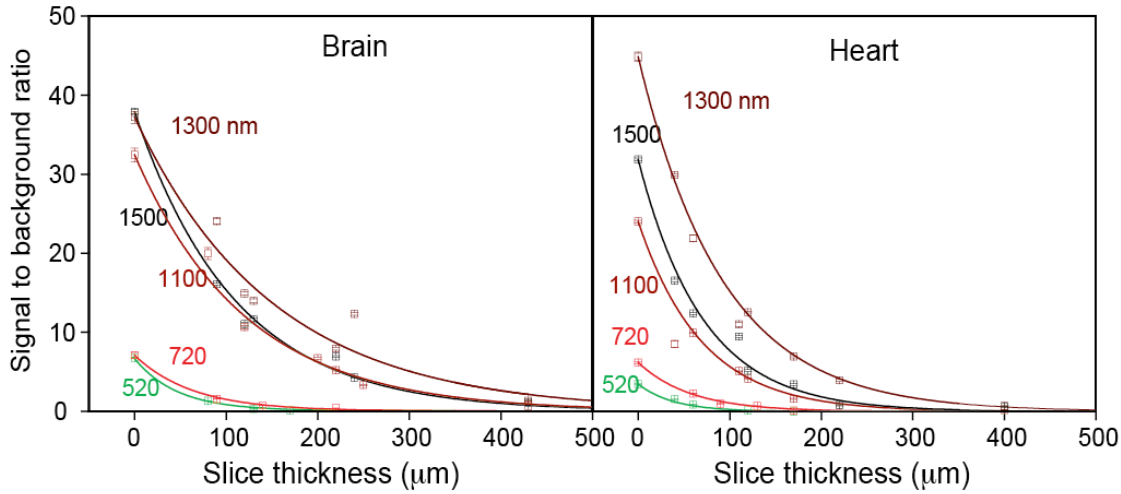

Fig. S5 The ratios of signal to background signals in the fluorescence images (Fig 6b in the text) of PbS/CdS QD-doped porous beads *versus* slice thickness of brain and heart.

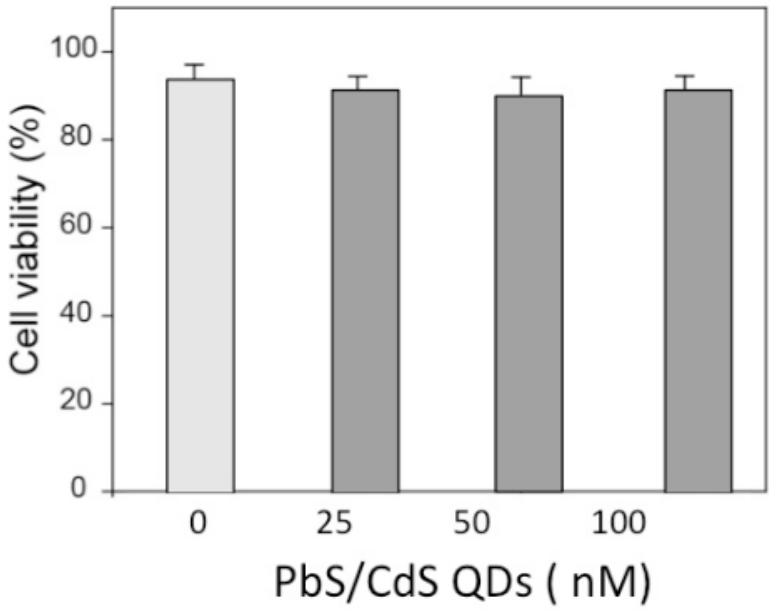

Fig. S6 Viability of HeLa cell for BSA-conjugated PbS/CdS QDs.